JMEPEG (2007) 16:63–67
DOI: 10.1007/s11665-006-9009-8
©ASM International
1059-9495/$19.00

Impact of Corrosion on Mass Loss, Fatigue and Hardness of BSt500$_S$ Steel

Ch.Alk. Apostolopoulos and D. Michalopoulos

(Submitted October 16, 2005; in revised form March 24, 2006)

The impact of corrosion on the properties of steel reinforcement in concrete structures was examined. An experimental investigation was carried out in order to gain better insight of the effect of corrosion on the mass loss, fatigue and hardness, of BSt500$_s$ 12 and 8 mm diameter steel bars that were artificially corroded in a Sodium Chloride environment for different corrosion levels. The fatigue limit of the 12 mm steel was reduced by 20–40% and the mass loss was 1.5–2.9% for 15 and 30 days corrosion level, while the mass loss of the 8 mm steel was 1.2–32% for 10–90 days corrosion. The hardness of the 8 mm steel was reduced by 25–35% and 2–10% in the outer and inner layers of the specimens for 30 and 60 days corrosion respectively. Corrosion created considerable reduction in the fatigue strength and life of the steel bars due to drastic drop in the energy density, formation of pitting and notches along with destruction of the hardest outer layer of martensite.

Keywords BSt500$_s$, energy density, fatigue, hardness, mass loss, salt spray corrosion

1. Introduction

Reinforced concrete structures exposed to oxygen and moisture are susceptible to corrosion of the reinforcing steel bars resulting in high repair cost. Corrosion is an electrochemical process during which metallic iron is converted to rust, creating volumetric expansion in the steel bars and also causing extremely high tensile forces within the concrete cover. This results in the formation of cracks from the steel bar to the surface or between the bars allowing oxygen and moisture to attack the bar faster and increase the corrosion rate. The rust reduces the bond strength and results in the loss of steel-concrete composite action, which affects the serviceability and performance of the structure (Ref 1–5).

The gradual degradation of the integrity of concrete structures is related to the accumulated detrimental effect of corrosion resulting in serious financial losses since corrosion causes concrete cracking and eventual deterioration of the structure before the end of its design life. Steel corrosion and associated cracking and spalling of concrete have been identified as the most severe form of deterioration. At rebar corrosion of about 7 and 12% the rib profile loss is around 45 and 70% accordingly, which explains the steel bar slippage mode of failure. Corrosion levels of 5 and 7% are observed to cause significant increase in crack width and rib profile loss (Ref 6, 7).

Ch.Alk. Apostolopoulos and **D. Michalopoulos,** Department of Mechanical Engineering and Aeronautics, University of Patras, Patras 26500, Greece. Contact e-mails: mixalop@mech.upatras.gr; capostalo@tee.gr.

In many seaside areas of Greece the climatic conditions constitute one of the most aggressive environments for concrete structures due to the severe ambient salinity, high temperature and humidity and also due to the ingress of chlorine through wind borne salt spray (Ref 8). Chloride induced damage of steel reinforcement results in concrete cracking and spalling, destruction of the protective barrier of steel and creation of steel pitting and cavities. Even though the impact of corrosion on the strength of steel is known, the current design codes do not face the problem since they are unable to quantify it and need further review. It has been attempted to quantify corrosion and mass loss of steel with the reduction of its mechanical properties (Ref 8). The repair cost for reinforced concrete bridges in the United States, due to soluble chlorides, is estimated to $8.3 billion (Ref 9, 10). Reinforced concrete structures are seriously affected by steel corrosion due to exposure to chlorides from seawater, salt and saltwater, deicing chemicals, brackish water, or spray from these sources (Ref 11, 12). The reduction in the structural performance of reinforced concrete members due to corroded steel is caused by the loss in the effective cross-sectional area of concrete due to cracking in the cover concrete and loss in the mechanical performance of bars due to reduction of their ductility and cross-sectional area (Ref 1, 8, 13).

The level of corrosion of steel bars affects their durability and performance and shortens the design life expectancy of structures (Ref 14–17). In the present study the impact of corrosion on mass loss, fatigue strength and hardness of steel was evaluated.

2. Experimental Work

2.1 Method and Testing Procedure

A series of tests were carried out on BSt500$_s$ tempcore steel, in order to qualitatively and quantitatively understand the effect of corrosion on steel bars and its properties. This material

contains C = 0.240%, P = 0.055%, S = 0.055%, and N = 0.013% in maximum permissible values of the final product and has mechanical properties as shown in Table 1. Tempcore is a patented mill process that produces high-strength reinforcing rebars via in line quenching and self-tempering.

Ribbed steel bars 12 and 8 mm in diameter were artificially corroded in a specially designed salt spray corrosion chamber, according to ASTM B117–94 standard, for 10, 20, 30, 45, 60, and 90 days. To accelerate corrosion the specimens were sprayed in a 5% sodium chloride and 95% distilled water solution, with pH range of 6.5–7.2 and spray chamber temperature of $35\pm\frac{1.1}{1.7}$ °C for different exposure times so that different corrosion levels were obtained. Pitting and notch formation was observed to have started progressively on the specimens after 10, 20 and 30 days corrosion, which became progressively more severe (Ref 8). After exposure the specimens were washed with clean water in order to remove any salt deposits from their surfaces and then dried. Several specimens were also exposed to salt spray for 10, 20 and 45 days respectively in order to monitor the evolution of corrosion damage and establish a calibration curve between salt spray exposure and corrosion level. The above materials and specific tests were selected since the 12 mm diameter bars are used as the main longitudinal reinforcement of structural elements and which are subjected to fatigue during earthquakes while the 8 mm bars are used for stirrups in the above structural elements and their mechanical properties are correlated to hardness.

For the 12 mm steel bars the mass loss and fatigue were measured and Woehler *S–N* diagrams and endurance limit graphs were constructed. The fatigue was measured on an MTS 250 kN servo hydraulic testing machine according to ISO/FDIS 15630-1 method using stress ratio $R = -1$ and frequency of 20 Hz. A total of 60 tests were performed in non-corroded and corroded specimens that had been exposed to salt spray for 15 and 30 days respectively. Twelve out of the 20 test points made per group were intended for the Woehler curves while the remaining eight were spares for unforeseen emergency. The minimum length had to be $14 \times d$, but the ones used were 280 mm long of which 55 mm length was used under each grip and 170 mm was the free length in order to facilitate loading in the testing machine.

Figure 1 shows a specially prepared cross section of an 8 mm diameter steel bar, where the high hardness martensite constituent is followed by a softer bainite and ferrite–pearlite layers. Micrographs of this material are shown in reference (Ref 8). For the 8 mm bars a total for 30 specimens were corroded at various levels from 10 to 90 days and the mass loss and hardness were measured. The hardness was measured on a Zwick 3212 Vickers hardness tester according to ASTM E92-82 standard. Rust cleaning was performed according to ASTM G 1-72 practice.

The actual degree of corrosion or corrosion level for both 12 and 8 mm specimens was measured as the mass loss of the bars before and after testing as follows:

Table 1 Mechanical properties of steel BSt500$_s$ specimen

Material	Yield stress, MPa	Tensile strength, MPa	Elastic modulus, GPa	Elongation, % (after breaking)
Ribbed bar	≥500	≥550	200	≥12

$$M_l = \frac{M_i - M_f}{M_i} \times 100 \qquad \text{(Eq 1)}$$

where M_l is the mass loss (%), M_i the mass of non-corroded specimen, M_f the mass of corroded specimen.

Figure 2 shows the mass loss variation of the corroded versus non-corroded 12 mm diameter steel specimens which is almost linear. The corresponding average cross sectional area A_s and the mass loss of the corroded bars are also indicated.

Figure 3 shows the mass loss variation of the corroded versus non-corroded 8 mm diameter steel specimens which up to 90 days appears increasing. It is assumed that the production of oxide layer around the specimen was uniform so that the results of Fig. 3 can be used to calculate the remaining diameter versus corrosion duration.

2.2 Fatigue Testing

Fatigue tests were carried out on 12 mm specimens at stress levels of ±325 MPa, ±265 MPa and ±200 MPa, for stress ratio $R = -1$ and frequency of 20 Hz. These tests were performed in order to determine the Woehler curves and endurance limit of the material. The average cross sectional area A_s of the specimens which remained after each corrosion treatment, and which was used in the calculation of the fatigue stress, was determined according to DIN 488-3 specification by:

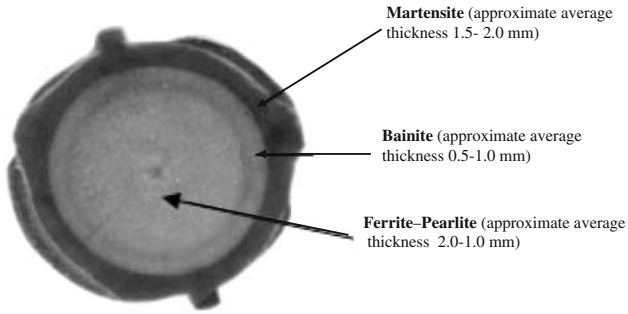

Fig. 1 Cross section of reinforcing steel bar type BSt500$_s$, 8 mm diameter

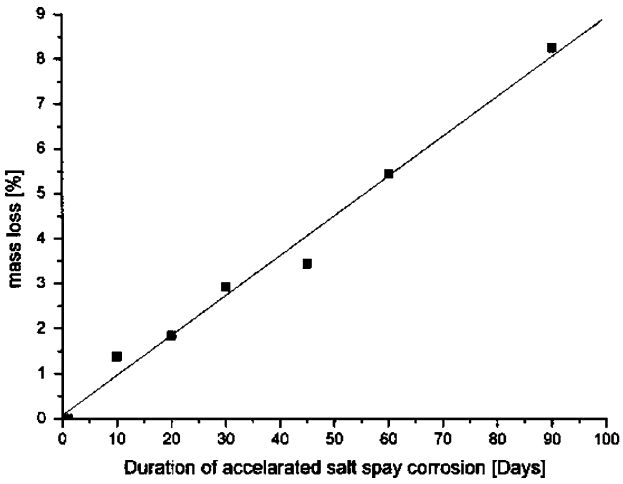

Fig. 2 Impact of corrosion on mass loss for 12 mm diameter specimens

$$A_s = \frac{1.274 \times G}{l} \qquad \text{(Eq 2)}$$

where A_s is the cross sectional area (cm^2), G the mass (g), l the length (mm) while the applied stress S was determined from the ratio of the applied force F and the cross sectional area A_s. This area had a definite influence on the fatigue strength since it was reduced as the corrosion duration increased. The rough outer surface of the corroded steel bars developed cavities, which made the average cross sectional area even smaller. These cavities were the source of stress concentration points and the start of the endurance limit reduction. During the fatigue testing the material undergoes cumulative damage, which is detrimental, and of much higher value in the cavities that have been developed through the corrosion process, resulting in much shorter life expectancy than the one that is measured through the uniform mass loss.

Woehler *S–N* diagrams for non-corroded and corroded for 15 and 30 days specimens, are shown in Fig. 4 displayed on logarithmic scale. The progressive reduction in fatigue strength can be realized as a function of the corrosion level. Woehler *S–N* diagrams are shown also in Fig. 5 for non-corroded and corroded steel specimens exposed to salt spray for 15 and 30 days, displayed on non-logarithmic scale. These curves are described satisfactorily with Weibull functions whose constants are shown in Table 2. It can be observed that for the same value of applied stress, of approximately 125 MPa, the expected steel life or cycles to failure decreases as a function of the salt spray exposure. The conventional fatigue limit of the material was determined for life expectancy of $N_f = 8.1 \times 10^6$ cycles.

Figure 6 shows the energy density or energy reserves as the area under the stress–strain curves, versus the degree of corrosion (Ref 8). It can be seen that as the exposure time to salt spray corrosion increases the energy density, the ductility properties and the breaking strength of the material decrease. In harsh environments and seismic areas the steel bar of reinforced concrete structures must have great amounts of energy density, which is a property characterizing the damage tolerance potential of a material and may be used to evaluate the fracture under both static and dynamic fatigue loading conditions (Ref 18). Figure 7 indicates the endurance limit for corroded versus non-corroded steel specimens exposed to salt spray for 15 and 30 days.

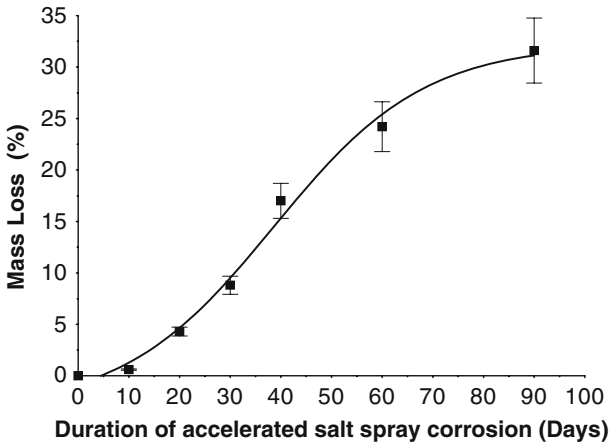

Fig. 3 Impact of corrosion on mass loss for 8 mm diameter specimens

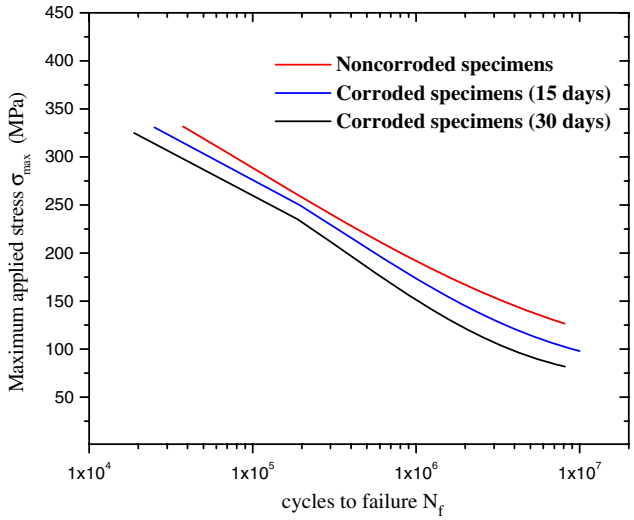

Fig. 4 Woehler *S–N* fatigue diagrams for non-corroded and corroded 12 mm diameter specimens

2.3 Hardness Testing

The hardness tests were performed on 8 mm steel specimens according to ASTM standards, on a Zwick 3212 Vickers hardness tester in a pattern shown in Fig. 8, using a 1.0 kg weight. Eleven different measurements were made across the diameter of each of the 10 specimens examined, at a distance d of 2.5 times the average diagonal of the indentation for non-corroded and corroded specimens. The corrosion level was 30 and 60 days respectively and five measurements were made on each specimen. Figure 9 shows the hardness distribution of each test point versus its location on the cross sectional area diameter.

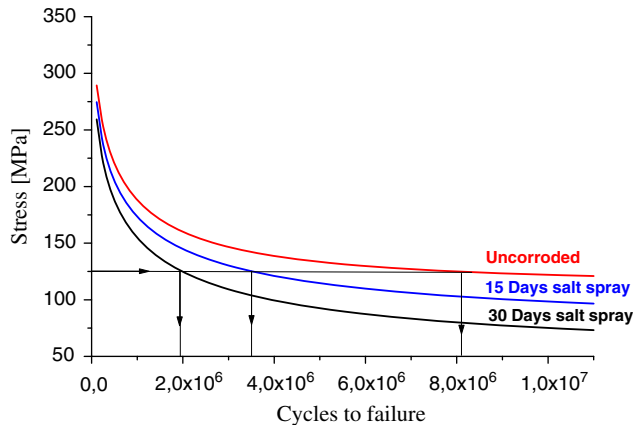

Fig. 5 Woehler *S–N* fatigue diagrams for non-corroded and corroded 12 mm diameter specimens

Table 2 Weibull constants

	Non-corroded	15 Days salt spray	30 days salt spray
C1	113.50884	75.97808	50.65955
C2	379.73621	401.14345	383.98002
C3	5.78098	5.78626	5.82995
C4	6.46082	5.16244	5.25499

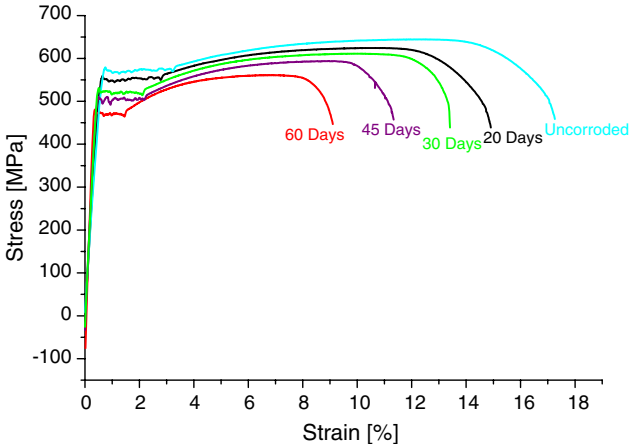

Fig. 6 Reduction of energy density for different corrosion levels for 12 mm diameter specimens

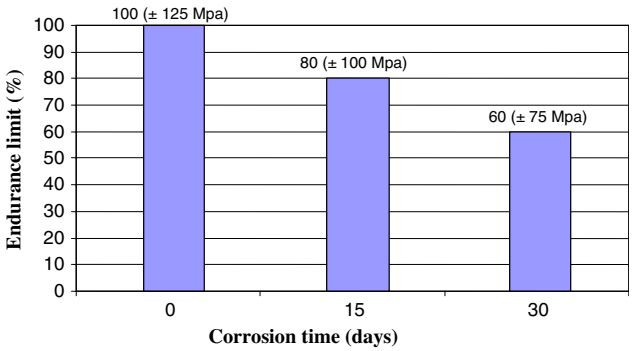

Fig. 7 Endurance limit variation versus time, for 12 mm diameter specimens

3. Results

Corrosion affected the integrity of steel and pitting became visible after a few days of salt spray, which became progressively more severe as the corrosion level increased. As the surface became rougher, cavities and notches were formed which reduced the specimen diameter locally.

Figure 2 shows that the mass loss, for 12 mm diameter specimens corroded for 10–90 days accordingly was approximately 1.37–8.26%. Figures 4 and 5 show that, for 12 mm bars, a small mass loss results in great reduction of strength and life expectancy. This is explained due to the pitting and formation of cavities and notches on the steel surface, which became more severe as the corrosion duration increased. The notches and pitting result in stress concentration points and acceleration of the effect of applied cyclic stresses and drastic drop in the energy density of the corroded steel (Ref 8). Small cracks usually form at points of stress concentration, which are propagated when the loads are repeated. The nominal fatigue limit of the material was established for life duration of $N_f = 8.1 \times 10^6$ cycles and Woehler S–N diagrams were constructed based on analytical relationships. During the corrosion process the hardest outer layer of martensite was affected the most, thus making the material weaker. Corrosion made the steel surface rougher and reduced locally its diameter. Fatigue failure was initiated from the outer surface and was transmitted

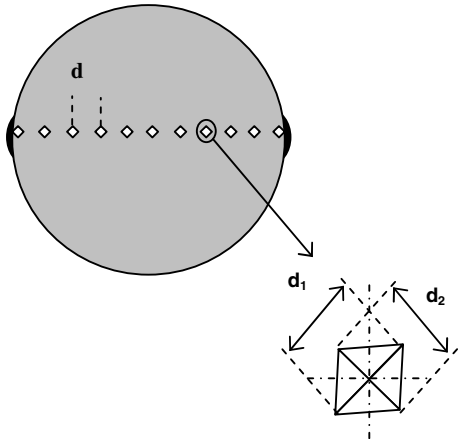

Fig. 8 Hardness testing across the cross sectional area of 8 mm diameter specimens

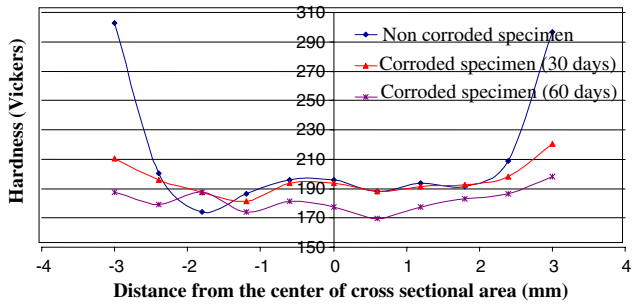

Fig. 9 Hardness tests for 8 mm diameter specimens

inwards. Thus points of stress concentration were developed which when combined with the reduction of ductility (energy density) and the loss of the martensite layer lead to a decrease of the useful life of steel. It can be seen also that for 12 mm diameter steel corroded for 15 and 30 days, which correspond to 1.5 and 2.9% mass loss, for a given applied stress for example 125 MPa and stress ratio $R = -1$, their life expectancy is reduced to 3.5×10^6 and 1.95×10^6 cycles respectively from 8.1×10^6 cycles of the non-corroded case, in other words the life expectancy of steel is reduced approximately by 56–76%. This is very significant for aggressive climatic conditions such as the ones existing in many coastal areas of Greece where salinity, high heat, humidity and earthquakes are the predominant factors. In such harsh environments the reinforcing steel bar of concrete structures need to have great amounts of energy density, which indicates their ability to absorb energy from external loads without danger of failure (Ref 18). Figure 6 shows that for 12 mm specimens the non corroded material has greater energy density than any of the corroded bars, as measured by the area under the stress–strain curve. A considerable decrease in energy density is observed as the duration of corrosion increased. In addition, after 2% corrosion level, the current design code for development length should be reviewed and additional studies are needed for verification and modification of the basic design principles. When engineers deal with seismic design they are mostly concerned with the mechanical property of energy density since this is described by the area under the stress–strain curve which includes also both the strength and ductility properties of the material. Also the

endurance limit was reduced by 20 and 40% accordingly for 15 and 30 days corrosion level as shown in Fig. 7.

Figure 3 shows that for corrosion level from 10 to 90 days the mass loss for 8 mm specimens was of the order of 0.60–31.86% accordingly. The difference in mass loss between 8 and 12 mm bars (Fig. 2 and 3) is due to the fact that for the same corrosion level both bars loose a layer of material of the same thickness X mm. Then the remaining percentage cross sectional area of the 8 mm bar will be smaller than the corresponding 12 mm bar. In other words for the 8 mm bar and the same corrosion level, the percentage mass loss will be greater than the corresponding 12 mm bar. The hardness distribution of the non-corroded specimens is higher in the outer part of the cross sectional area and is reduced as it gets closer to the center as shown in Fig. 8 and 9. This is justified since the outer part is composed of hard martensite, followed by softer bainite and even softer ferrite–pearlite as shown also in Fig. 1. It can also be observed that overall the non-corroded steel specimens are harder than the corroded bars. The hardness of the corroded steel was reduced by 25–35% and 2–10% in the outer and inner diameters of the specimens for 30 and 60 days corrosion duration accordingly. The greatest reduction takes place in the outer part of the specimens where corrosion seems to destroy the martensite layer. This is also confirmed from Fig. 6 where the yield strength, which is also related to the hardness of the material, is lowered. Since 8 and 12 mm BSt500$_s$ steel specimens are materials of the same category and the same microstructure, their mechanical properties are the same (Ref 8). As corrosion progresses it is observed that further reduction in hardness towards the outer part of the specimens takes place. No significant reduction of hardness is observed towards the center of the specimen, which indicates that corrosion does not appear to influence it. For the non-corroded specimens the high hardness at 3 mm from the center is justified since this is still in the martensite area.

4. Conclusions

An experimental study was conducted in order to evaluate the impact of corrosion on the mass loss, fatigue and hardness of 12 and 8 mm diameter steel specimens and the following conclusions are drawn:

1. For the 12 mm specimens:

(a) The mass loss for 10–90 days corrosion duration was found to be of the order the 1.37–8.26% respectively.
(b) Corrosion was initiated at the base of the ribs and as it progressed the ribs were worn down. At 90 days the average height of the ribs was reduced by approximately 80–85%.
(c) The fatigue limit of the corroded specimens was reduced due to reduction of the exterior hard layer of martensite and drastic drop in the energy density. The endurance limit was reduced by 20% and 40% accordingly for 15 and 30 days corrosion level while the mass loss was 1.5 and 2.9% respectively.

2. For the 8 mm specimens:

(a) The mass loss for 10–90 days corrosion duration was found to be of the order of 0.60–31.86% accordingly.
(b) Corrosion was initiated at the base of the ribs and as it progressed the ribs were worn down. At 90 days the average height of the ribs was reduced by approximately 85%.
(c) The hardness of the non-corroded steel is greater in the outer part of the cross sectional area and is reduced as it gets closer to the center due to the hard martensite, followed by the softer bainite and ferrite–pearlite layers. The hardness of the corroded steel was reduced by 25–35% and 2–10% in the outer and inner diameters of the specimens for 30 and 60 days corrosion. The greatest reduction appears to take place in the outer part of the specimens where corrosion seems to destroy the martensite layer.

References

1. C. Fang, K. Lundgren, L. Chen, and C. Zhu, Corrosion Influence on Bond in Reinforced Concrete, *Cement Concrete Res.*, 2004, **34**, p 2159–2167
2. G.J. Al-Sulaimani, M. Kaleemullah, I.A. Basunbul, and Rasheeduzzafar, Influence of Corrosion and Cracking on Bond Behaviour and Strength of Reinforced Concrete Members, *Proc. A.C.I.*, 1990, **2**, p 220–231
3. X. Fu and D.D.L. Chung, Effect of Corrosion on the Bond between Concrete and Steel Rebar, *Cement Concrete Res.*, 1997, **27**(12), p 1811–1815
4. R. Capozucca, Damage to Reinforced Concrete due to Reinforcement Corrosion, *Constr. Build. Mater.*, 1995, **9**(5), p 295–303
5. Z.P. Bazant, Physical Model for Steel Corrosion in Concrete Sea Structures-Theory, J. Struct. Div., June 1979, p 1137–1153
6. A.A. Almusallam, A.S. Al-Gahtani, A.R. Aziz, and Rasheeduzzafar, Effect of Reinforcement Corrosion on Bond Strength, *Constr. Build. Mat. J.*, 1996, **10**(2), p 123–129
7. A.A. Almusallam, A.S. Al-Gahtani, A.R. Aziz, F.H. Dakhil, and Rasheeduzzafar, Effects of Reinforcement Corrosion on Flexural Behavior of Concrete Slabs, *J. Mat. Civil Eng.*, 1996, **8**(3), p 123–127
8. Ch. Alk. Apostolopoulos, M.P. Papadopoulos, and Sp.G. Pantelakis, Tensile Behavior of Corroded Reinforcing Steel Bars BSt 500s, *Constr. Build. Mater.*, 2006, **20**, p 782–789
9. G.C. Koch, M.P. Brongers, M.P. Thompson, Y.P.Virmani, and J.H. Payer, Corrosion Costs and Preventive Strategies in the United States, Federal Highway Administration, Washington, D.C, report No. FHWA-RD, 2002, p 1–156
10. G.G. Clementa, Testing of Selected Metallic Reinforcing Bars for Extending the Service Life of Future Concrete Bridges, Final report, Virginia Transportation Research Council, Charlottesville, VA, VTRC 03-R7, 2002
11. X. Wang and X. Liu, Bond Strength Modelling for Corroded Reinforcements, *Constr. Build. Mater.*, 2006, **20**, p 177–186
12. L. Chung, S.-H. Cho, J.-H. Jay Kim, and S.-T. Yi, Correction Factor Suggestion for ACI Development Length Provisions based on Flexural Testing of RC Slabs with Various Levels of Corroded Reinforced Bars, *Eng. Struct.*, 2004, **26**, p 1013–1026
13. J.G. Cabrera, Deterioration of Concrete due to Reinforcement Steel Corrosion, *Cement Concrete Compos.*, 1996, **18**(l), p 47–59
14. P. Schiessl Corrosion of Steel in Concrete. RILEM Report TC 60-CSC, 1988
15. K. Stanish, R.D. Hooton, and S.J. Pantazopoulou, Corrosion Effects on Bond Strength in Reinforced Concrete, *ACI Struct. J.*, 1999, **96**(6), p 915–921
16. H.S. Lee, T. Noguchi, and F. Tomosawa, Evaluation of the Bond Properties between Concrete and Reinforcement as a Function of the Degree of Reinforcement Corrosion, *Cement Concrete Res.*, 2002, **32**(8), p 1313–1318
17. Cabrera, J.G., and Ghoddoussi, P., Effect of Reinforcement Corrosion on the Strength of the Steel Concrete Bond. Int. Conf., Bond in Concrete—from Res. to Pract., Vol. 3, Riga, Latvia, 1992, p 10.11–10.24
18. G.C. Sih and C.K. Chao, Failure Initiation in Unnotched Specimens Subjected to Monotonic and Loading, *Theor. Appl. Fract. Mech.*, 1984, **2**, p 67–73